Electronic structure of a Si δ-doped layer in a GaAs/$Al_xGa_{1-x}As$/GaAs quantum barrier

J. M. Shi
COBRA, Interuniversitair Onderzoekinstituut, Afdeling Technische Natuurkunde, Technische Universiteit Eindhoven, P.O. Box 513, NL-5600 MB Eindhoven, The Netherlands and Departement Natuurkunde, Universiteit Antwerpen (UIA), Universiteitsplein 1, B-2610 Antwerpen, Belgium

P. M. Koenraad and A. F. W. van de Stadt
COBRA, Interuniversitair Onderzoekinstituut, Afdeling Technische Natuurkunde, Technische Universiteit Eindhoven, P.O. Box 513, NL-5600 MB Eindhoven, The Netherlands

F. M. Peeters
Departement Natuurkunde, Universiteit Antwerpen (UIA), Universiteitsplein 1, B-2610 Antwerpen, Belgium

J. T. Devreese
Departement Natuurkunde, Universiteit Antwerpen (UIA), Universiteitsplein 1, B-2610 Antwerpen, Belgium and COBRA, Interuniversitair Onderzoekinstituut, Afdeling Technische Natuurkunde, Technische Universiteit Eindhoven, P.O. Box 513, NL-5600 MB Eindhoven, The Netherlands

J. H. Wolter
COBRA, Interuniversitair Onderzoekinstituut, Afdeling Technische Natuurkunde, Technische Universiteit Eindhoven, P.O. Box 513, NL-5600 MB Eindhoven, The Netherlands

(Received 10 November 1995; revised manuscript received 4 April 1996)

We present a theoretical study of the electronic structure of a heavily Si δ-doped layer in a GaAs/$Al_xGa_{1-x}As$/GaAs quantum barrier. In this class of structures the effect of DX centers on the electronic properties can be tuned by changing the $Al_xGa_{1-x}As$ barrier width and/or the Al concentration, which leads to a lowering of the DX level with respect to the Fermi energy without disturbing the wave functions much. A self-consistent approach is developed in which the effective confinement potential and the Fermi energy of the system, the energies, the wave functions, and the electron densities of the discrete subbands have been obtained as a function of both the material parameters of the samples and the experimental conditions. The effect of DX centers on such structures at nonzero temperature and under an external pressure is investigated for three different models: (1) the DX^0_{nc} model with no correlation effects, (2) the d^+/DX^0 model, and (3) the d^+/DX^- model with inclusion of correlation effects. In the actual calculation, influences of the background acceptors, the discontinuity of the effective mass of the electrons at the interfaces of the different materials, band nonparabolicity, and the exchange-correlation energy of the electrons have been taken into account. We have found that (1) introducing a quantum barrier into δ-doped GaAs makes it possible to control the energy gaps between different electronic subbands; (2) the electron wave functions are more spread out when the repellent effect of the barriers is increased as compared to those in δ-doped GaAs; (3) increasing the quantum-barrier height and/or the application of hydrostatic pressure are helpful to experimentally observe the effect of the DX centers through a decrease of the total free-electron density; and (4) the correlation effects of the charged impurities are important for the systems under study. [S0163-1829(96)06135-8]

I. INTRODUCTION

Two-dimensional electron systems have attracted a lot of attention in the past decade because of the interesting physics that were observed in them, and because of their device applications.[1,2] In δ-doped structures a two-dimensional electron gas (2DEG) can be formed with a much higher free-electron density as compared to the modulation doped heterostructures,[3,4] and a higher electron mobility as compared to bulk-doped semiconductors.[5] These are important effects for applications in high-speed electronics[6] and in optoelectronic devices.[7] From a fundamental point of view, δ-doped structures are very interesting because one can study the interaction between the electrons and charged impurities in the limit of very strong coupling and in the case of multisubband transport.

In the case that DX centers saturate the electron density, correlation effects in the charge distribution in the doping layer are expected to be present.[8–10] δ-doped structures are ideal to study these correlation effects because of the strong interaction between the charged impurities and the free electrons. In this paper we propose a structure in which one can tune the influence of correlations on the transport properties of a 2DEG.

In order that DX centers, and thus correlations in the charge distribution, have any influence on the transport properties, the Fermi level (E_F) has to be resonant with the DX level. It is a well known effect that DX centers in $Al_xGa_{1-x}As$ are resonant with the Γ band at an Al fraction of approximately 0.25 or at a hydrostatic pressure of 20 kbar in GaAs.[11] Chadi and Chang[12] have put forward the general

idea that deep centers, like the DX center, follow the averaged conduction band because these deep, strongly localized centers sample the whole dispersion relation. In GaAs, the DX level is positioned at least 200 meV above the conduction-band minimum, and can be made resonant with the Fermi level either by raising the Fermi level or by lowering the DX level. The Fermi level can be raised by increasing the doping concentration.[13] But in order to reach $E_F \geq 200$ meV, such high doping concentrations are needed that usually self-compensation occurs.[14] An alternative approach is to lower the position of the DX level relative to the conduction band by the application of hydrostatic pressure or by increasing the Al fraction in the structure.[8] However, in GaAs a hydrostatic pressure of at least 20 kbar is needed to push the DX level below the Fermi level. Here we will use barrier δ-doped GaAs structures, in which we can tune the position of the DX level relative to the Fermi level in such a way that one needs only a modest hydrostatic pressure to push the DX level through the Fermi level even in samples with a small Fermi energy. This should facilitate a better access to δ-doped structures where correlations in the charge distribution occur.

Bulk semiconductor structures containing a δ-doped layer have already been investigated extensively.[15–20] Zrenner *et al.*[8] extended these works to study the saturation of the free carrier concentration in δ-doped GaAs. The DX level was modeled as a neutral deep donor having a fixed energy with *no correlation* effects ($d^+ + e \rightarrow DX^0_{\rm nc}$). Taking this energy level as a fitting parameter, they were able to explain the saturation of the free-electron density with increasing doping concentration and pressure.[21] Using a Monte Carlo simulation, Sobkowicz, Wilamowski, and Kossut[10] generalized the above calculations to include the effects of the charge distribution in δ-doped GaAs within two different models: in the d^+/DX^0 model the dopants give rise to either a positively charged shallow (d^+) donor or a neutral deep ($d^+ + e \rightarrow DX^0$) donor, and in the d^+/DX^- model the dopants give rise to either a positively charged shallow donor or a negatively charged deep ($d^+ + 2e \rightarrow DX^-$) donor. The correlation effects of the charged impurities were also shown in a doped heterostructure,[22] bulk-doped GaAs,[9] and δ-doped n-i-p-i superlattices.[23] The electronic structure of a δ-doped quantum well was investigated in Ref. 24, but effects due to the DX centers were neglected. In the absence of a δ-doped layer, Peeters and co-workers[25] have shown a strong influence of introducing positive barriers (wells) into the wells (barriers) of a superlattice on its electronic structure. This provides an effective and realistic tool to control the energy gaps between the different minibands.

In this paper, we investigate structures where a Si δ-doped layer is located at the center of a GaAs/$Al_xGa_{1-x}As$/GaAs quantum barrier. Such structures can provide three useful advantages as compared to normal δ-doped GaAs: (1) The influence of the barrier on the different subbands is various. This makes it possible to control the energy gaps between the electron subbands. (2) Due to the repellent effect of the barrier on the electrons, they are ''pushed'' away from the impurities. Consequently the electron mobility of the system is expected to be enhanced. (3) Because the Si dopants reside in the $Al_xGa_{1-x}As$ barrier and the energy position of the DX center relative to the conduction band depends on the Al fraction, one can tune the difference between the DX and Fermi levels easily. This is the most important advantage we will discuss in this work. Therefore samples can be grown which have a different fraction of their ''free'' electrons trapped on DX centers, whereas other electronic parameters of the samples, e.g., the shape of the wave functions, are hardly changed. Also, the hydrostatic pressure needed to change the fraction of electrons trapped on DX centers can be modest and tuned to an accessible experimental range of pressures. Thus correlation effects on, for instance, the mobility can be studied in detail. DX centers have a similar behavior in GaAs and $Al_xGa_{1-x}As$, except that the energy separation between the DX level and the Γ-band minimum differs. However, the electronic structure in these two systems can be various due to a different population of the DX centers.[13] By solving the coupled Schrödinger and Poisson equations of the system, the wave functions, confined energy levels, and electron population of the subbands will be obtained as well as the one-dimensional (1D) effective confinement potential and the Fermi energy. Diffusion of the donors along the growth direction is assumed to be uniform in a sheet with a finite thickness. In the present calculation, effects of the discontinuity of the electronic effective mass at the interfaces between two materials, band nonparabolicity, the background acceptors, and the exchange-correlation interaction of the electrons have been included. In order to study the influence of the DX centers on the electronic properties of the system, three models are discussed at non-zero temperature and under hydrostatic pressure in the absence ($DX^0_{\rm nc}$) (Ref. 8) and the presence (d^+/DX^0 and d^+/DX^-) (Ref. 10) of spatial correlations in the charge distribution. For the latter case we discuss only narrow δ-doped layers, such that correlations between charged impurities can be described within a model of zero width of the δ-doped layer. We have found the following. (1) Increasing the quantum-barrier height and/or applying hydrostatic pressure are helpful to experimentally observe the effects of the DX centers through a decrease of the total free-electron density. (2) The electron wave functions are more spread out when increasing the barrier height, and the presence of DX centers changes the carrier density and the arrangement and/or number of charged impurities. These effects should influence the electron mobility. (3) The correlation effects of the charged impurities are important for describing the system under study.

This paper is organized as follows. In Sec. II a self-consistent approach for the electronic structure of a δ-doped quantum barrier is presented in the absence of the DX centers. Inclusion of the DX centers without any correlations is discussed for nonzero temperature, and in the presence of hydrostatic pressure in Sec. III. We assumed that the DX centers freeze out at $T = 100$ K.[26] Below this temperature, transfer of electrons from the DX bound states to the conduction band becomes impossible. The spatial correlation effects in the charge distribution are introduced in Sec. IV, where we will discuss samples with very narrow δ-doped layers. Our conclusions and discussions are presented in Sec. V.

II. ELECTRONIC STRUCTURE OF A δ-DOPED QUANTUM BARRIER

We will describe a Si δ-doped layer located at the center of a GaAs/$Al_xGa_{1-x}As$/GaAs quantum barrier, as is shown

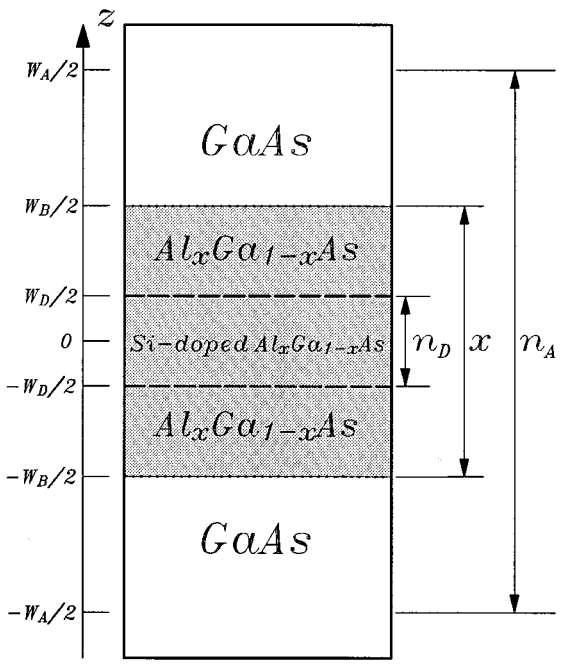

FIG. 1. Schematic diagram of the proposed structure: a Si δ-doped layer in a GaAs/$Al_xGa_{1-x}As$/GaAs quantum barrier. W_D, W_B, and W_A are the widths for the Si-doped layer with 3D doping concentration n_D, the $Al_xGa_{1-x}As$ quantum barrier whose height depends on the Al concentration x, and the acceptor region with 3D concentration n_A, respectively.

in Fig. 1. The z direction is along the growth axis. The quantum barrier consists of a $Al_xGa_{1-x}As$ sheet with width W_B sandwiched between two bulk GaAs layers. The central region of the barrier is uniformly and heavily doped with Si atoms over a thickness W_D at a three-dimensional (3D) concentration n_D. Typically one has 2D doping densities $N_D=n_DW_D\sim10^{12}$ cm^{-2}, at which the donors have an average distance less than the effective Bohr radius in GaAs. As a consequence, a positively charged layer is constructed, which provides a 1D confinement potential for electrons in the z direction. For a typical p-type background (3D) concentration of $n_A=10^{14}$ cm^{-3}, a depletion layer of 4.45 μm ($=W_A/2$) (Ref. 19) is formed at each side of the doping layer.

Within the single-particle approximation, assuming the system to be uniform in the xy plane, and excluding any effects due to the DX centers, the Hamiltonian describing the free electrons of the 2DEG is reduced to

$$\left[-\frac{d}{dz}\frac{\hbar^2}{2m^*(z)}\frac{d}{dz}+U_{\rm EFF}(z)\right]\Psi_I(z)=E_I\Psi_I(z), \quad (1)$$

where E_I is the energy of the Ith electronic subband described by the normalized wave function $\Psi_I(z)$; $m^*(z)$ is the electron effective mass:[27] in GaAs, $m^*(z)/m_e=0.067$ and in the $Al_xGa_{1-x}As$ barrier $m^*(z)/m_e=0.067+0.083x$; and $U_{\rm EFF}(z)$ is the 1D effective confinement potential for the electrons which consists of three contributions

$$U_{\rm EFF}(z)=U_B(z)+U_C(z)+U_{\rm XC}(z), \quad (2)$$

where $U_B(z)=0.6(1.155x+0.37x^2)\Theta(W_B/2-|z|)$ in units of eV (Ref. 27) describes the quantum barrier, and $\Theta(z)$ is a step function; $U_C(z)$ is the Hartree potential determined by the Poisson equation

$$\frac{d^2U_C(z)}{dz^2}=\frac{4\pi e^2}{\epsilon_0}[n_D\Theta(W_D/2-|z|)-n_A\Theta(W_A/2-|z|)-n_e(z)], \quad (3)$$

with $n_e(z)=\Sigma_I n_I(z)$ the electron charge density determined through

$$n_I(z)=|\Psi_I(z)|^2\int_{E_I}^{\infty}f(E,T,E_F)D(E,k_I)dE, \quad (4)$$

where $f(E,T,E_F)=[1+e^{(E-E_F)/k_BT}]^{-1}$ is the Fermi-Dirac distribution function with E_F the Fermi energy, and $D(E,k_I)$ the density of states in each subband which includes the effect of band nonparabolicity[28] through the electron energy E and the average wave vector $k_I=[\int_{-\infty}^{\infty}|d\Psi_I(z)/dz|^2dz]^{1/2}$. Furthermore, charge conservation requires that

$$N_D=N_e+N_A, \quad (5)$$

where $N_A=n_AW_A$ is the 2D acceptor concentration, and $N_e=\Sigma_I N_I$ the areal density of the 2DEG with $N_I=\int_{-\infty}^{\infty}dz\,n_I(z)$ the electron density in the Ith subband. $U_{\rm XC}(z)$ results from the exchange-correlation effects of the electron gas, and will be expressed by a simple analytic parametrization[29]

$$U_{\rm XC}(z)=-\sqrt[3]{18/\pi^2}\frac{R_y^*}{r_s}[1+0.0545r_s\ln(1+11.4r_s^{-1})], \quad (6)$$

with $r_s=[4\pi n_e(z)/3]^{-1/3}/a_B^*(z)$, and $a_B^*(z)=\hbar^2\epsilon_0/m^*(z)e^2$ the effective Bohr radius, where $\epsilon_0=13.0$ is the dielectric constant of the system, and $R_y^*=e^2/2\epsilon_0a_B^*(z)$ the effective Rydberg. $U_{\rm XC}(z)$ may be discontinuous at interfaces between GaAs and $Al_xGa_{1-x}As$ due to the different effective electron masses. The potential $U_{\rm EFF}(z)$ depends on $n_e(z)$ via $U_{\rm XC}(z)$ $[U_C(z)]$ through $r_s(z)$ $[n_e(z)]$, while $n_e(z)$ depends on $U_{\rm EFF}(z)$ via $\Psi_I(z)$ through Eq. (1). Therefore, the above set of equations describing the system has to be solved self-consistently.

Figure 2 shows the wave functions of the three lowest electron subbands along the z direction at $T=0$ K for a δ-doped layer, with $N_D=5\times10^{12}$ cm^{-2} and $W_D=20$ Å, in quantum barriers having widths of (a) $W_B=20$ Å, (b) $W_B=50$ Å, and (c) $W_B=100$ Å, and heights of $x=0.0$ (solid), $x=0.1$ (dotted), $x=0.2$ (dash-dotted), and $x=0.3$ (dashed curves). The following are clear: (1) The repellent effect of the barriers on the wave functions is more pronounced with increasing barrier height, which should result in an enhancement of the electron mobilities. (2) In the case of a fixed barrier height, this effect becomes stronger at first, and then becomes weaker with increasing barrier width, because the system is changing from 3D GaAs to a quantum barrier structure, and then to 3D $Al_xGa_{1-x}As$ (see $x=0.2$). (3) The influence of the barrier on the symmetric states

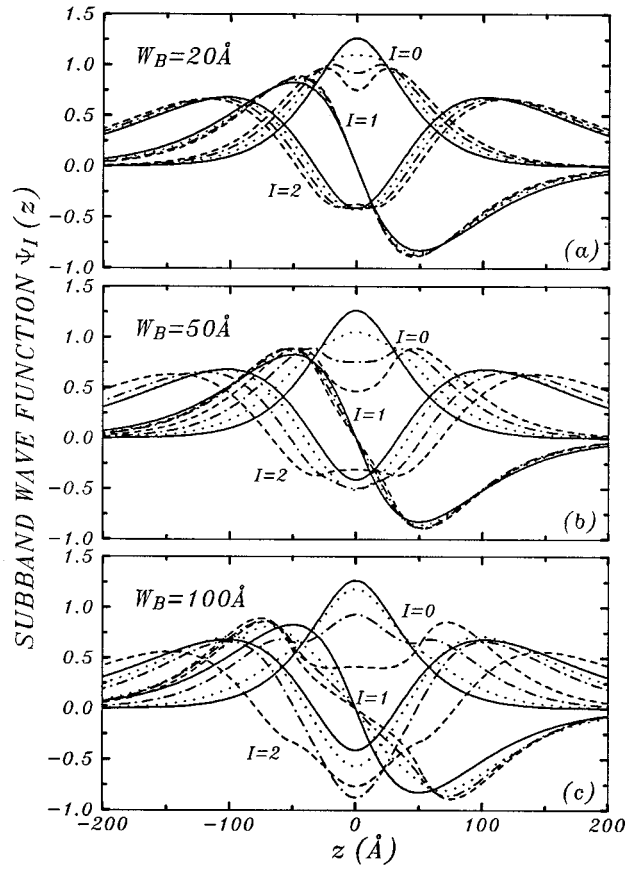

FIG. 2. Wave functions of the three lowest electronic subbands along the z direction at $T=0$ K for a δ-doped layer with 2D doping concentration $N_D=5\times10^{12}$ cm^{-2} and doping width $W_D=20$ Å located at the center of the quantum barriers of widths (a) $W_B=20$ Å, (b) $W_B=50$ Å, and (c) $W_B=100$ Å, and heights $x=0.0$ (solid), $x=0.1$ (dotted), $x=0.2$ (dash-dotted), and $x=0.3$ (dashed curves).

($I=0$ and 2) is stronger than that on the antisymmetric state ($I=1$), due to the fact that electrons in the symmetric states are closer to the barrier.

The total effective potential $U_{\rm EFF}(z)$ is plotted in Fig. 3 together with the energy levels of the four lowest subbands at $T=0$ K for a δ-doped quantum barrier with fixed $N_D=5\times10^{12}$ cm^{-2}, $W_D=20$ Å , $W_B=50$ Å, and four different barrier heights (a) $x=0.0$, (b) $x=0.1$, (c) $x=0.2$, and (d) $x=0.3$, where all energies are relative to the Fermi energy E_F. Increasing barrier height will change dramatically the positions of the energy levels. As a consequence, a quasidegeneracy [see Fig. 3(d)] for E_0 and E_1 (also for E_2 and E_3) can be reached. This behavior is similar to bonding and antibonding states in two coupled quantum wells. Thus one is able to control the energy gaps between the different subbands with the help of quantum barriers. This is consistent with the conclusions of Ref. 25.

The dependence of the energy gaps between the electron subbands on the parameters of the quantum barrier is illustrated in Fig. 4, where we plot the energy levels [Figs. 4(a) and 4(c)] and the electron densities [Figs. 4(b) and 4(d)] of the four lowest subbands for δ-doped quantum barriers with $N_D=5\times10^{12}$ cm^{-2} and $W_D=20$ Å. The left figures are for the case of a fixed width ($W_B=50$ Å) and changing barrier height, and the right figures for the case of a fixed height ($x=0.15$) and changing barrier width. The electron population in the symmetric states ($I=0$ and 2) decreases with increasing barrier height except at low Al concentration for $I=2$, while it increases in the antisymmetric states [see Figs. 4(a) and 4(b)]. The dependence on the barrier width in the case of a fixed height is complicated, since the system is going from 3D GaAs to a quantum-barrier structure, and finally to 3D $Al_xGa_{1-x}As$.

III. EFFECTS OF THE UNCORRELATED *DX* CENTERS

By now it is well established[11] that many donors in III-V semiconductors have to be described by the coexistence of a shallow donor state and a deep donor state. By the application of hydrostatic pressure, Zrenner *et al.*[8] have shown that *DX* centers influence the electronic properties of δ-doped GaAs. Here, their work will be generalized to the present structures. In normal δ-doped GaAs the *DX* level is high above the Fermi energy. However, due to the presence of the quantum barrier and/or the use of hydrostatic pressure, the *DX* level and the Fermi energy can easily become resonant. In this section we assume that the Si donors in the *DX* state are neutral and have no interaction ($DX^0_{\rm nc}$ model). In our calculations, the energy of the *DX* centers is described by

$$E_{DX}(z)=\alpha+\beta T+\gamma P+\eta x\Theta(W_B/2-|z|)+U_{\rm EFF}(z), \quad (7)$$

where T is fixed at 100 K, P is the hydrostatic pressure, and the four coefficients (α, β, γ, and η) are given by $\alpha=300$ meV ($E_{DX}-E_\Gamma$ in GaAs at $P=0$ and $T=0$), $\beta=-0.15$ meV/T $[d(E_{DX}-E_\Gamma)/dT]$, $\gamma=-10$ meV/kbar $[d(E_{DX}-E_\Gamma)/dP]$, and $\eta=-700$ meV $[d(E_{DX}-E_\Gamma)/dx$ in $Al_xGa_{1-x}As]$, which are in the region of values reported in the literature.[9,30–33] The 2D density of the $DX^0_{\rm nc}$ donors is given by

$$N_{DX}=\frac{N_D-N_A}{W_D}\int_{-W_D/2}^{W_D/2}\left[1+\frac{1}{g}\exp\left(\frac{E_{DX}(z)-E_F}{k_BT}\right)\right]^{-1}dz \quad (8)$$

with $g=2$ the *DX*-level degeneracy.[34] Including the *DX* centers in the charge conservation equation (5), we obtain

$$N_D=N_e+N_{DX}+N_A. \quad (9)$$

With the modifications mentioned above the set of equations describing the electronic structure are solved self-consistently.

In Fig. 5 we plot the energy levels (a) relative to the Fermi energy, and electron densities (b) of the four lowest subbands of a δ-doped layer ($N_D=1\times10^{13}$ cm^{-2}, $W_D=20$ Å) in quantum barriers with a fixed width ($W_B=20$ Å) as a function of the barrier height at $T=100$ K. The total free-electron density (N_e, long dashed) and the density of the $DX^0_{\rm nc}$ donors (N_{DX}, dot-dot-dot-dashed curves) are also shown in Fig. 5(b). It is clear that more *DX* centers become populated with increasing barrier height. Due to the population of $DX^0_{\rm nc}$ states, the dependence of the electronic structure on the barrier height is quite dif-

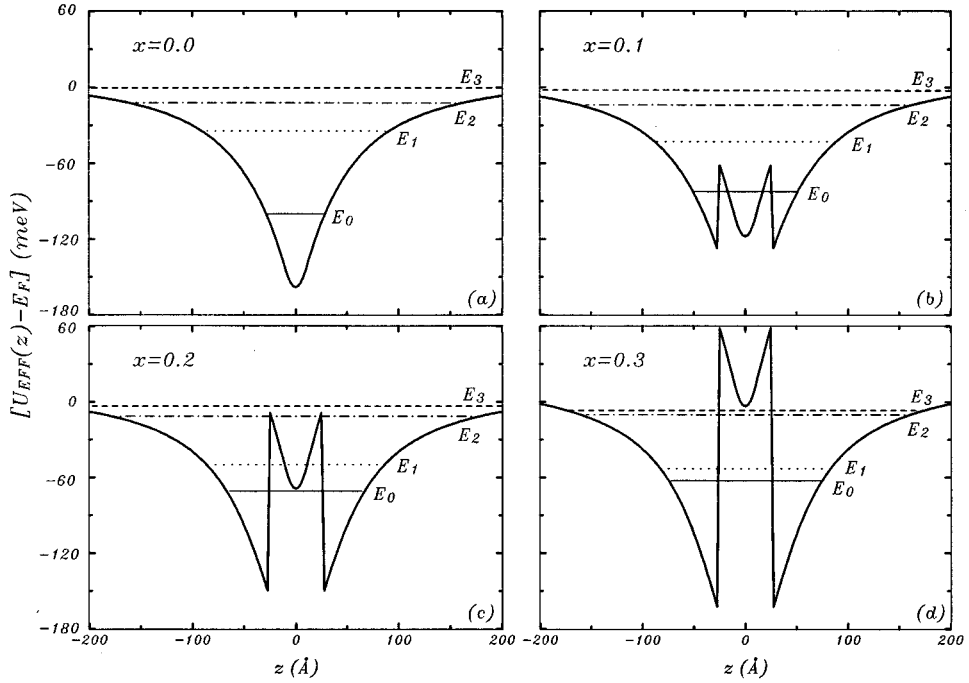

FIG. 3. Difference between the Fermi energy and the total effective potential in real space along the z axis at $T=0$ K for a δ-doped layer with doping concentration $N_D=5\times10^{12}$ cm^{-2} and doping width $W_D=20$ Å in quantum barriers of width $W_B=50$ Å and Al concentration (a) $x=0.0$, (b) $x=0.1$, (c) $x=0.2$, and (d) $x=0.3$. The four lowest subband energy levels are also plotted.

ferent from the previous calculations when the DX centers are excluded. This can be seen by a qualitative comparison with Figs. 4(a) and 4(b).

The use of hydrostatic pressure[26] provides a useful tool to determine the properties of the DX centers in $Al_xGa_{1-x}As$ compounds because their energy position is lowered with respect to the Fermi energy. In Fig. 6 the total areal density of free electrons N_e is displayed, together with the population of the DX^0_{nc} donors, as a function of external pressure for a δ-doped layer with $N_D=5\times10^{12}$ cm^{-2} and $W_D=40$ Å in GaAs (solid) and in $W_B=40$-Å quantum barriers with $x=0.05$ (dotted), $x=0.10$ (dash dotted), $x=0.15$ (dashed), and $x=0.20$ (long-dashed curves) at $T=100$ K. Notice that at low pressures ($P<7.5$ kbar), the population of the DX level is relatively small; however, by increasing pressure the DX state becomes more populated. This results in a decrease of the free-electron density. As we have proposed, indeed, the population of the DX centers is enhanced by the presence of the quantum barriers and/or the application of hydrostatic pressure.

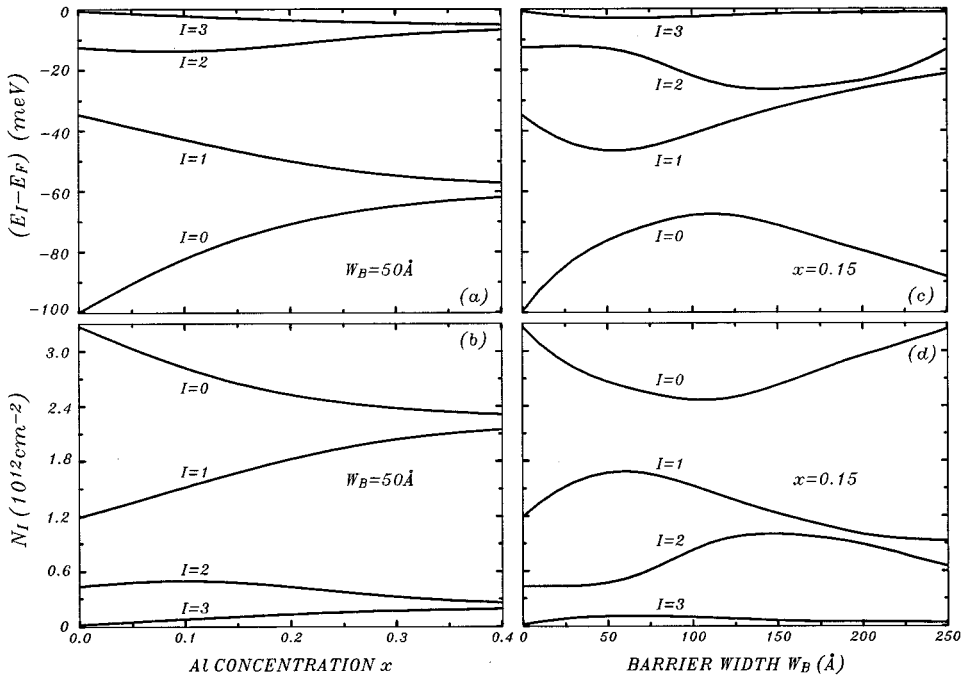

FIG. 4. Energies relative to the Fermi level [(a) and (c)] and electron densities [(b) and (d)] of the four lowest subbands as a function of the barrier height (Al concentration x) [(a) and (b)] with fixed barrier width $W_B=50$ Å, and of the barrier width with fixed barrier height $x=0.15$ [(c) and (d)] for the structures with fixed doping strength $N_D=5\times10^{12}$ cm^{-2} and doping width $W_D=20$ Å at $T=0$ K.

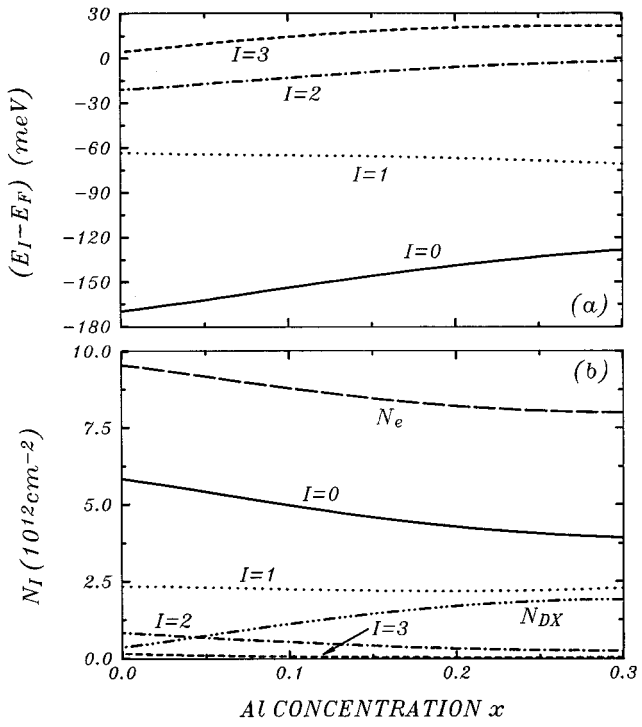

FIG. 5. Dependence of the energy levels relative to the Fermi energy (a) and the electron densities (b) of the four lowest subbands on the barrier height for a δ-doped layer with doping density $N_D=1\times10^{13}$ cm^{-2} and doping width $W_D=20$ Å in quantum barriers with fixed barrier width $W_B=20$ Å at $T=100$ K and $P=0$ kbar. The neutral-donor density N_{DX} and the total free-electron density N_e are also plotted in (b).

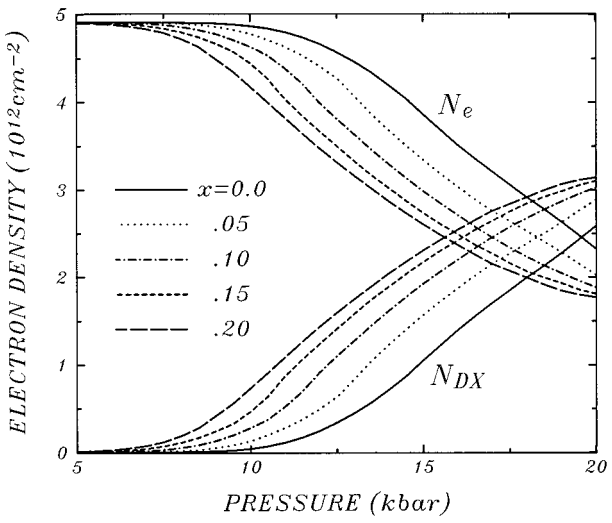

FIG. 6. Pressure dependence of the free-electron density N_e and the neutral-donor density N_{DX} for a δ-doped layer with doping concentration $N_D=5\times10^{12}$ cm^{-2} and doping width $W_D=40$ Å in quantum barriers with fixed barrier width $W_B=40$ Å and five different barrier heights $x=0.0$ (solid), $x=0.05$ (dotted), $x=0.10$ (dot dashed), $x=0.15$ (dashed), and $x=0.20$ (long-dashed curves) at $T=100$ K.

IV. CORRELATION EFFECTS OF THE CHARGED IMPURITIES

A random spatial distribution of donors in a δ-doped layer results in a random distribution of positive charges when all dopants are ionized. When *part* of the donors are ionized, spatial correlations in the distribution of charged impurities can result due to the Coulomb interaction between them. The charges (electrons) trapped by the dopants are distributed in such a way that the total energy of the system is minimized through the correlation energy $\mathbf{E_c}$ [per unit area (volume) in 2D (3D)]. These correlation effects will change the electronic structure of the system, as has been shown clearly for both bulk-doped[9] and δ-doped GaAs.[10] Now we will include them in our δ-doped quantum barrier structures. Since it is still not clear which of the two models, the d^+/DX^0 model or the d^+/DX^- model, is applicable, we will discuss both of them. The equilibrium condition of the reservoirs of filled DX centers and the 2DEG for both models is given by

$$E_F(N_e)=E_{DX}-\frac{d\mathbf{E_c}}{dN_{\rm tot}}, \tag{10}$$

where $N_{\rm tot}=N_e+N_A$ is the net charge density in the δ-doped layer. This equation shows us that it is possible for some of the electrons to occupy the DX state, even if E_{DX} is higher than E_F at zero temperature. Equation (10), together with charge neutrality and Eqs. (1)–(4) and (6), will determine the electronic structure of the system.

In the d^+/DX^0 model the impurities are either in the DX^0 state or in the d^+ state. Thus one may expect that positively charged centers would be as far away from each other as possible. This can be described in the short-range interaction model by a pair-correlation function

$$g_{++}(r)=\Theta(r-r_c), \tag{11}$$

where r_c is the correlation radius which is determined by $N_{\rm tot}$ and N_D through the Poisson distribution[35]

$$N_{\rm tot}V_c=1-\exp(-N_DV_c), \tag{12}$$

where $V_c=\pi r_c^2$ for 2D ($4\pi r_c^3/3$ for 3D). In the d^+/DX^- model, the impurities exist either in the d^+ state or in the DX^- state. In order to describe correlations between the $(++)$, $(--)$, and $(+-)$ charge pairs, one must define three pair-correlation functions[9] given by

$$g_{++}(r)=C_{++}\Theta(r_c-r)+\Theta(r-r_c), \tag{13a}$$

$$g_{+-}(r)=C_{+-}\Theta(r_c-r)+\Theta(r-r_c), \tag{13b}$$

$$g_{--}(r)=\Theta(r-r_c), \tag{13c}$$

where $C_{++}=\{(N_DV_c)^2-2[N_DV_c-1+\exp(-N_DV_c)]\}/(N_+V_c)^2$ and $C_{+-}=[N_DV_c-1+\exp(-N_DV_c)]/N_+N_-V_c^2$ with $N_\pm=\frac{1}{2}(N_D\pm N_{\rm tot})$ the densities of the d^+ and DX^- centers respectively. Since the positions of all the impurities are random, these three functions must obey the following equation

$$N_+^2g_{++}(r)+2N_+N_-g_{+-}(r)+N_-^2g_{--}(r)=N_D^2. \tag{14}$$

The equation for r_c in this model is given by

$$N_- V_c = 1 - (1 + N_D V_c)\exp(-N_D V_c). \tag{15}$$

Notice that both Eqs. (12) and (15) are valid for 2D and 3D, with $N_{\rm tot} \sim N_D$,[10,9] which restricts the range of applicability of the theory. To the best of our knowledge, there is no analytical formula to describe charged-impurity correlations in a quasi-2D structure. Therefore we will only investigate very narrow δ-doped layers, such that the theory for the 2D system will be a good approximation. The structure for which this approximation is valid must meet $r_c < W_D$, where r_c is calculated for 3D. Equation (15) does not have any nontrivial solution for $N_{\rm tot}/N_D < 0.403\,18$,[10] beyond which we have used $r_c = \{[3.823 - 9.339 N_{\rm tot}/N_D + 8.210(N_{\rm tot}/N_D)^2 - 2.693(N_{\rm tot}/N_D)^3]/\pi N_D\}^{1/2}$, which is able to give results very close to the solutions of Eq. (15) in its solvable region, and a corresponding expression for bulk-doped GaAs (Ref. 9) has been proven to be successful for the whole region of $N_{\rm tot}/N_D$.

The exact description of the Coulomb interaction between charged impurities in our structure is quite difficult due to screening by the quasi-2DEG. In the present work, we have used a Yukawa potential determining the interaction between any two (i and j) impurities

$$U_{i,j}(|\vec{r}_i - \vec{r}_j|) = \frac{q_i q_j}{\epsilon_0 |\vec{r}_i - \vec{r}_j|} \exp\left(-\frac{|\vec{r}_i - \vec{r}_j|}{\lambda}\right), \tag{16}$$

where q_i denotes the charge of the i center ($q_i = e$ or 0 for d^+/DX^0, and $q_i = \pm e$ for d^+/DX^-), and λ is the screening length given by the semiclassical, 3D Thomas-Fermi (3DTF) screening theory. It was found that for δ-doped GaAs,[36,37] the interaction depends weakly on the actual value of λ, where $\lambda = 50$ Å was taken for 2D. In general, considering quasi-2D structures with strong quantization and inhomogeneous electron distribution in the z direction, it is essential to use a quantum-mechanical screening theory like the random-phase approximation.[23] The argument for using 3DTF screening theory in the present work is based on the large average width of the free-electron layer in the system. For typical δ-doped structures, the widths of these layers are wider than 150 Å, which are significantly larger, than the screening length.[10] Otherwise, this theory will overestimate the screening. The following expression[9] has been used in the present work for the screening length λ:

$$\lambda = \left(\frac{\pi \epsilon_0 \hbar^2}{4 e^2 m^* k_F}\right)^{1/2}, \tag{17}$$

which depends on the free-electron density through the Fermi wave vector k_F. Using the pair-correlation functions and the Yukawa potential, one is able to obtain the correlation energy $\mathbf{E_c}$ for the d^+/DX^0 model

$$\mathbf{E_c} = \frac{\pi e^2 \lambda}{\epsilon_0} N_{\rm tot}^2 \left[\exp\left(-\frac{r_c}{\lambda}\right) - 1\right], \tag{18}$$

and, for the d^+/DX^- model,

$$\mathbf{E_c} = \frac{\pi e^2 \lambda}{\epsilon_0} (N_{\rm tot}^2 + N_D^2) \left[\exp\left(-\frac{r_c}{\lambda}\right) - 1\right]. \tag{19}$$

By solving Eq. (10) the electronic structure of the system will be obtained with the inclusion of the correlation effects of the charged impurities. A detailed comparison of the free-electron density for a δ-doped layer with $N_D = 5 \times 10^{12}$ cm^{-2} and $W_D = 40$ Å at $T = 100$ K has been performed for the cases of (a) $\lambda \equiv 50$ Å,[37] (b) $\lambda = [\pi \epsilon_0^3 \hbar^6 / 192 e^6 m^{*3} n_e(0)]^{1/6}$,[23] and (c) Eq. (17).[9] We found that all three models with three different λ values give almost the same results for this sample, which is consistent with the conclusion of Refs. 36 and 37. But for δ-doped quantum barriers, it is found that model (b) gives results which deviate from those of the other models when the barrier height is increased, which is due to the small $n_e(0)$.

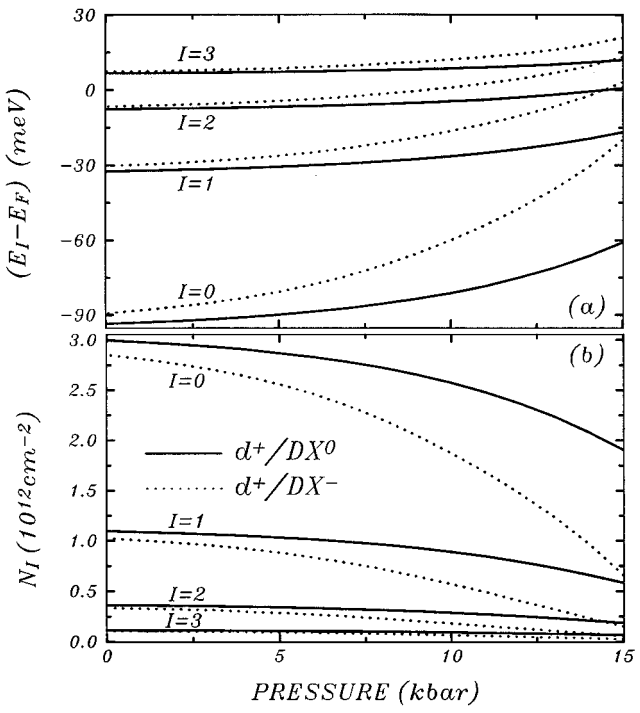

FIG. 7. Dependence of the energy levels relative to the Fermi energy (a) and the electron densities (b) of the four lowest subbands on external pressure for a δ-doped GaAs with doping density $N_D = 5 \times 10^{12}$ cm^{-2} and doping width $W_D = 40$ Å at $T = 100$ K within the d^+/DX^0 (solid) and d^+/DX^- (dotted curves) models.

In Fig. 7 we depict (a) the position of the energy level relative to the Fermi energy, and (b) the electron density of the four lowest subbands of a δ-doped GaAs with $N_D = 5 \times 10^{12}$ cm^{-2} and $W_D = 40$ Å at $T = 100$ K as a function of hydrostatic pressure in the d^+/DX^0 (solid) and d^+/DX^- (dotted curves) models. At low pressure ($P < 5$ kbar), the effects of the charged-impurity correlations are relatively small, while at high pressure ($P > 5$ kbar) these effects strongly influence the energies and electron densities of the subbands. The d^+/DX^- model gives stronger correlation effects than the d^+/DX^0 one because the gain in interaction energy is much larger when making a close pair of donors with opposite charges (d^+ and DX^-), as compared to making a close pair consisting of a DX^0 center and a d^+ center. A distinction between these two models is thus possible in the high-pressure region. We should keep in mind that $N_{\rm tot} = 0$ implies there are no correlations in the d^+/DX^0 model because $N_+ = 0$. However, correlations in the situation still exist in the d^+/DX^- model because $N_+ = N_- = N_D/2$.

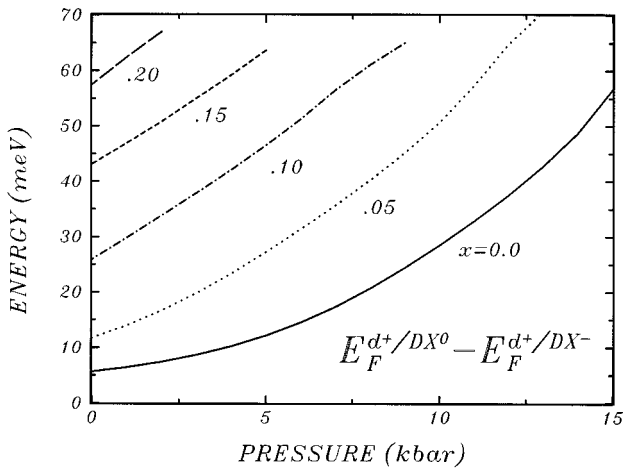

FIG. 8. Fermi-energy difference between the d^+/DX^0 and d^+/DX^- models as a function of external pressure at $T=100$ K for the same structures as those shown in Fig. 6.

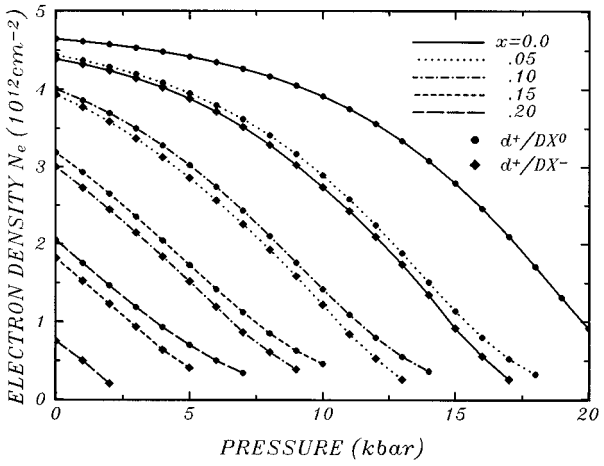

FIG. 9. Calculated total free-electron density vs pressure at $T=100$ K within the d^+/DX^0 (curves with circles) and d^+/DX^- (curves with diamonds) models for the same systems as those shown in Fig. 6.

The Fermi-energy difference between the d^+/DX^0 and d^+/DX^- models is depicted in Fig. 8 as a function of external pressure at $T=100$ K for the same structures as those shown in Fig. 6. Notice that (1) the Fermi energy in the d^+/DX^0 model is always higher than that in the d^+/DX^- model, which is due to the stronger correlation effects in the latter model; (2) this difference increases with increasing barrier height, which again shows stronger effects of DX centers than those in δ-doped GaAs; and (3) the difference in Fermi energy results from the difference in $d\mathbf{E_c}/dN_{\rm tot}$ between the two models. The absolute value of this difference can be taken as a measurement for the size of the correlation effects.

Comparison of the total free-electron density N_e as a function of external pressure between the d^+/DX^0 (curves with circles) and d^+/DX^- (curves with diamonds) models is given in Fig. 9 for the same structures as those in Figs. 6 and 8. It is clear that with increasing barrier height and/or pressure the free-electron density decreases. The d^+/DX^- model gives a lower electron density than the d^+/DX^0 model due to its stronger correlation effects. We expect that the correlation effects must influence the electron mobility because (1) in the d^+/DX^0 model the number of scatterers is less than those in the $DX^0_{\rm nc}$ model (see Fig. 6) for the same situation; and (2) in the d^+/DX^- model the d^+ and DX^- centers try to form dipoles, which makes the scattering potential less effective. Recently, we performed a calculation of the quantum mobility of electrons in δ-doped GaAs in the presence of an applied pressure, which shows the importance of the correlation effects clearly.[38] It is interesting to note that the results for the d^+/DX^- model are very close to those for the d^+/DX^0 model when we replace the Al concentration x by $x+0.05$. However, one cannot compare 10 kbar of hydrostatic pressure with 10% of Al as is usually done,[8] because our system is no longer a bulklike structure.

V. CONCLUSIONS AND DISCUSSIONS

Using a self-consistent approach, we calculated the electronic structure of a δ-doped layer in a quantum-barrier system and obtained useful physical quantities, some of which are experimentally observable, such as N_I and N_e. The strong influence of the barrier on the electronic properties of a 2DEG was clearly demonstrated, which can provide an effective method to control the energy gaps of the system. Effects of the DX centers on the system were investigated in the absence and presence of spatial correlation of the charged impurities at nonzero temperature and under an external presure. This shows the increased importance of such correlation effects in the present structures with increasing barrier height and pressure.

At present it is premature to draw quantitative conclusions concerning which of the three DX models is applicable because of the following: (1) The results depend on accurate measurements of the coefficients in Eq. (7). For example, the values of α reported in the literature vary from 160 to 320 meV, and α differs from sample to sample but also from the theoretical model which was used to analyze the data.[30,9] (2) There exist other mechanisms, e.g., self-compensation of the Si impurities in the δ-doped layer, which either partially or totally give rise to a saturation of the free-electron concentration. We have demonstrated that the effects of DX centers are more pronounced in the present structures because the difference between the DX level and the Γ-band minimum decreases, and therefore experiments on such structures should give valuable information on the impact of such DX centers to their electronic properties.

ACKNOWLEDGMENTS

One of us (F.M.P.) was supported by the Belgian National Science Foundation. J.M.S. wishes to thank the Technology University Eindhoven (The Netherlands) for financial support. J.T.D. acknowledges support by the Belgian National Science Foundation (NFWO, No. G.0287.95). Part of this work was performed by the Phantoms Network of Excellence ESPRIT-III BRA Action 7360.

[1] T. Ando, A.B. Fowler, and F. Stern, Rev. Mod. Phys. **54**, 437 (1982).
[2] G. Bastard, *Wave Mechanics Applied to Semiconductor Heterostructures* (Les Editions de Physique, Les Ulis, France, 1988).
[3] S.J. Bass, J. Cryst. Growth **47**, 613 (1979).
[4] C.E.C. Wood, G. Metze, J. Berry, and L.F. Eastman, J. Appl. Phys. **51**, 383 (1980).
[5] E.F. Schubert, J.E. Cunningham, and W.T. Tsang, Solid State Commun. **63**, 591 (1987).
[6] E.O. Göbel and K. Ploog, Prog. Quantum Electron. **14**, 289 (1990).
[7] G.H. Döhler, Phys. Status Solidi **52**, 79 (1972).
[8] A. Zrenner, F. Koch, R.L. Williams, R.A. Stradling, K. Ploog, and G. Weimann, Semicond. Sci. Technol. **3**, 1203 (1988).
[9] J. Kossut, Z. Wilamowski, T. Dietl, and K. Świątek, Acta Phys. Pol. A **79**, 49 (1991).
[10] P. Sobkowicz, Z. Wilamowski, and J. Kossut, Semicond. Sci. Technol. **7**, 1155 (1992).
[11] P.M. Mooney, J. Appl. Phys. **67**, R1 (1990).
[12] D.J. Chadi and K.J. Chang, Phys. Rev. Lett. **61**, 873 (1988); Phys. Rev. B **39**, 10 063 (1989).
[13] P.M. Koenraad, in *Delta Doping of Semiconductors*, edited by E.F. Schubert (Cambridge University Press, London, 1995), p. 304.
[14] P.M. Koenraad, I. Bársony, J.C.M. Henning, J.A.A.J. Perenboom, and J.H. Wolter, in *Semiconductor Interfaces at the Sub-Nanometer Scale*, edited by H.W.M. Salemink and M.D. Pashley (Kluwer, Dordrecht, 1993), p. 35.
[15] See, e.g., *Delta Doping of Semiconductors* (Ref. 13).
[16] G.Q. Hai, N. Studart, and F.M. Peeters, Phys. Rev. B **52**, 8363 (1995); **52**, 11 273 (1995); G.Q. Hai and N. Studart, *ibid.* **52**, R2245 (1995).
[17] A. Zrenner, F. Koch, and K. Ploog, Surf. Sci. **196**, 671 (1988).
[18] M.H. Degani, Phys. Rev. B **44**, 5580 (1991).
[19] P.M. Koenraad, A.C.L. Heessels, F.A.P. Blom, J.A.A.J. Perenboom, and J.H. Wolter, Physica B **184**, 221 (1993).
[20] P.M. Koenraad, A.F.W. van de Stadt, J.M. Shi, G.Q. Hai, N. Studart, P. Vansant, F.M. Peeters, J.T. Devreese, J.A.A.J. Perenboom, and J.H. Wolter, Physica B **211**, 462 (1995).
[21] S.P. Wilks, A.E. Cornish, M. Elliott, D.A. Woolf, and R.H. Williams, J. Appl. Phys. **76**, 3583 (1994).
[22] E. Buks, M. Heiblum, and H. Shtrikman, Phys. Rev. B **49**, 14 790 (1994).
[23] C. Metzner, K. Schrüfer, U. Wieser, M. Luber, M. Kneissl, and G.H. Döhler, Phys. Rev. B **51**, 5106 (1995).
[24] W. Xu and J. Mahanty, J. Phys. Condens. Matter **6**, 4745 (1994).
[25] F.M. Peeters and P. Vasilopoulos, Appl. Phys. Lett. **55**, 1106 (1989); P. Vasilopoulos, F.M. Peeters, and D. Aitelhabti, Phys. Rev. B **41**, 10 021 (1990).
[26] R. Piotrzkowski, T. Suski, P. Wiśniewski, K. Ploog, and J. Knecht, J. Appl. Phys. **68**, 3377 (1990).
[27] H.J. Lee, L.Y. Juravel, J.C. Wolley, and A.J. Springthorpe, Phys. Rev. B **21**, 659 (1980).
[28] U. Rössler, Solid State Commun. **49**, 10 943 (1984).
[29] O. Gunnarson and B.I. Lundqvist, Phys. Rev. B **13**, 4274 (1976).
[30] P.M. Koenraad, W. de Lange, F.A.P. Blom, M.R. Leys, J.A.A.J. Perenboom, J. Singleton, and J.H. Wolter, Semicond. Sci. Technol. **6**, B143 (1991).
[31] P.M. Mooney, T.N. Theis, and E. Calleja, J. Electron. Mater. **20**, 23 (1991).
[32] Z. Wilamowski, J. Kossut, W. Jantsch, and G. Ostermeyer, Semicond. Sci. Technol. **6**, B38 (1991).
[33] R.A. Stradling, E.A. Johnson, A. Mackinnon, R. Kumar, E. Skuras, and J.J. Harris, Semicond. Sci. Technol. **6**, B137 (1991).
[34] T.N. Theis, P.M. Mooney, and S.L. Wright, Phys. Rev. Lett. **60**, 361 (1988).
[35] E.V. Chenskii and Yu. Ya. Tkach, Zh. Éksp. Teor. Fiz. **79**, 1809 (1980) [Sov. Phys. JETP **52**, 915 (1980)].
[36] K. Świątek, T. Dietl, Z. Wilamowski, and J. Kossut, in *Proceedings of 19th International Conference on Physics of Semiconductors*, edited by W. Zawadzki (Institute of Physics, Warsaw, 1988), p. 1571.
[37] P. Sobkowicz, Z. Wilamowski, and J. Kossut, J. Phys. Condens. Matter **5**, 5283 (1993).
[38] J.M. Shi, P.M. Koenraad, A.F.W. van de Stadt, F.M. Peeters, J.T. Devreese, and J.H. Wolter, in *Proceedings of the 23rd International Conference on the Physics of Semiconductors*, edited by M. Scheffler and R. Zimmermann (World Scientific, Singapore, 1996).